

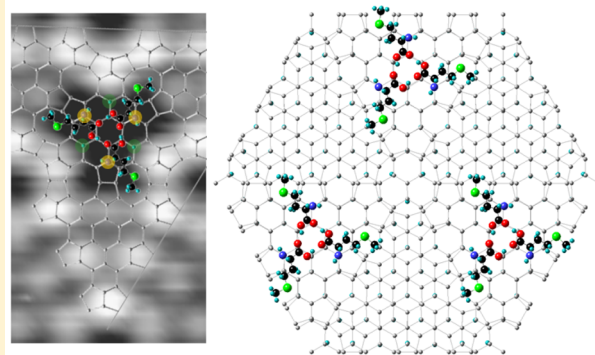
Self-Organized Supported Clusters of L-Methionine

Fatemeh R. Rahsepar and K. T. Leung*

WATLab and Department of Chemistry, University of Waterloo, Waterloo, Ontario N2L 3G1, Canada

S Supporting Information

ABSTRACT: Fundamental understanding of self-organization and integration of biomaterials on semiconductors is essential to the development of biological electronic devices. While formation of supramolecular structures by hydrogen bonding and/or electrostatic forces appears common on metal surfaces, the availability of dangling bonds on semiconductor surfaces introduces new bonding mechanisms that could disrupt the self-organization of basic biomolecules. Here, we demonstrate self-organization of L-methionine on Si(111)7×7 at room temperature into a Y-shaped trimer, as the first “perfect-match” supported cluster reported to date. The Y trimer is found to be securely attached within the 7×7 half unit cell and is driven by intralayer hydrogen bonding among the unattached carboxylic acid groups in a ring configuration. Its unique cluster structure is verified by ultra-large-scale density functional theory calculations with van der Waals corrections. The Y trimer (key) offers a remarkably stable “lock-and-key” fit to the 7×7 unit cell (lock) for biofunctionalization and molecular templating.



■ INTRODUCTION

Basic interactions of various types of organic molecules with semiconductor surfaces have attracted much attention in the past two decades. This has led to a wide range of applications in the design and fabrication of hybrid organic–inorganic electronic devices, particularly in the functionalization and molecular processing of silicon substrates.^{1,2} With the availability of a wide variety of functional groups, organic molecules offer not only powerful chemical and physical properties but also potential biological functionality. Of all the semiconductors, silicon is the best known substrate for fabricating electronic devices because of its unique electronic and surface properties, with Si(111)7×7 and Si(100)2×1 being two of the most studied semiconductor surfaces to date. With 18 directional dangling bonds (at 6 center and 6 corner electrophilic adatom sites, and 6 nucleophilic restatom sites) plus one dangling bond shared among the four corner-hole sites per unit cell,³ the Si(111)7×7 surface provides a highly reactive surface for adsorption of both inorganic and organic materials. Since the landmark observation of the 7×7 surface reconstruction with atomic resolution⁴ by scanning tunnelling microscopy (STM)⁵ shortly after its invention, adsorption of a wide variety of organic molecules on Si(111)7×7 have been studied by STM. These include small organic molecules with a single functional group to larger biomolecules with multiple functional groups. These molecules have provided a rich test bed for investigating not just molecule–surface reactions but also surface-mediated intermolecular processes such as molecular self-organization.

Based on STM observation of organic molecules (with different functional groups) chemisorbed on both the

nucleophilic and electrophilic sites of the 7×7 surface, the molecule–surface interactions can be categorized into four general types of reactions: (a) [2+2]-like cycloaddition or di- σ binding, (b) [4+2]-like or Diels–Alder cycloaddition, (c) covalent attachment via dissociative chemisorption, and (d) formation of dative-bond adducts. Early STM studies of acetylene⁶ and ethylene⁷ adsorption showed a [2+2]-like product di- σ bonded on a pair of adjacent Si adatom–restatom sites. Similarly, quad- σ bonded products on two neighboring pairs of adjacent adatom–restatom sites were found for several aliphatic dienes, including 1,6-heptadiene, 1,7-octadiene and 1,13-tetradecadiene.⁸ These [4+2] cycloaddition products have been observed for unsaturated hydrocarbon (1,3-butadiene⁹) at adatom–adatom pairs, and for aromatic hydrocarbons^{10–13} and toluene¹¹, aromatic heterocycles (thiophene^{14,15}), and DNA base (thymine¹⁶) at adjacent adatom–restatom pairs. These STM studies showed that the center adatom was more reactive with these organic molecules than the corner adatom. Moreover, a wide range of covalent attachments, from nitroxyl free radicals,¹⁷ aromatic molecules (pyrrole,¹⁸ naphthalene,¹⁹ tetracene,²⁰ and pentacene²¹), and amines (dimethylamine²²) to benchmark amino acids (glycine,²³ alanine, and cysteine²⁴) and peptide (glycylglycine²⁵), have also been investigated by STM. These molecules were found to react with adjacent adatom–restatom pairs, usually with the dissociated hydrogen atom bonded at a nearby restatom site. Finally, STM studies showed that donating the lone-pair charge density of the N

Received: November 29, 2015

Revised: February 28, 2016

Published: March 3, 2016

atom in one of DNA bases (adenine²⁶) and amines (trimethylamine²²) to the Si atom could lead to long-range dative bonding. In addition to direct bonding of the aforementioned neutral organic moieties to various Si surface sites, adsorption and nanoscale patterning of zwitterionic molecular films on the Si(111)7×7 surface has also been reported.²⁷

Of all the organic and biological molecules, amino acids represent the building blocks of proteins and peptides. Understanding their adsorption on and interactions with semiconductor surfaces enables the use of biofunctionalization to convert a potentially hostile inorganic surface, such as silicon, to a more biologically friendly substrate. Such biofunctionalization is important because it is often the first step in building a biocatalyst or biodevice. Of the 20 amino acids, methionine (COOHCH₂CH(NH₂)CH₂CH₂SCH₃) is one of two sulfur-containing aliphatic amino acids. Methionine contains a terminal thiol ether (–CH₂SCH₃) group, unlike the other sulfur-containing amino acid, cysteine, that contains a thiol (–SH) group. As an essential amino acid, methionine plays several important roles in cell metabolism in the human body, and an abnormal level of methionine could indirectly cause a variety of health problems. The adsorption of L-methionine on the Si(111)7×7 surface is therefore of particular interest to not just surface science but also biomedical research. Among the large volume of work on organic molecules on metal surfaces,²⁸ there are only a few studies of methionine, all of which focused on its self-assembly on single-crystal metal surfaces. On Au(111),^{29,30} D- and L-methionine were found to form parallel chain or zipperlike dimer rows in the formation of hydrogen-bonded zwitterionic layer at room temperature. L-Methionine was reported to form nanogratings by self-assembly with tunable periodicity in the zwitterionic chemical state on a Ag(111) surface held at 320 K during deposition.³¹ Furthermore, steering chiral organization of L-methionine on Cu(111)³² was found to be strongly affected by the substrate reactivity and thermal activity. To distinguish between self-assembly and self-organization, the interplay between molecular flux and surface diffusivity should be considered. If the flux of incident molecules is low and the diffusivity is high such that the adsorbates could freely diffuse on the surface, the growth of thermodynamically equilibrated structures at appropriate bonding sites is favored, resulting in self-assembly. On the other hand, if the flux is high and diffusivity is low, the molecules could not reach the thermodynamically favored sites and get trapped in a diffusion-limited state (e.g., at a local minimum of the potential energy surface), which would lead to self-organization.³³ Unlike metal surfaces, the availability of directional dangling bonds on Si(111)7×7 could play a significant role in changing the nature of surface functionalization that involves strong bonding in neutral form, resulting in reduced diffusivity and in formation of self-organized patterns, in marked contrast to metal surfaces on which the zwitterionic form is the norm. This offers a new paradigm in manipulating the formation and evolution of surface chemical bonds of these building-block biomolecules, and in taking advantage of surface-mediated hydrogen bonding for nanolithography and sensing applications.

Here, we study for the first time the early growth stage of L-methionine, from monomers to dimers and trimers, on Si(111)7×7 at room temperature under ultrahigh vacuum condition by high-resolution STM imaging. We illustrate the formation of a unique Y-shaped trimer through self-organization of three methionine molecules, each bonded to

a Si adatom through its dehydrogenated amino group. Using large-scale ab initio quantum-mechanical calculations, based on the density functional theory (DFT) with van der Waals corrections (D2), we provide precise structural models for the observed methionine features, including the “delta or Δ-shaped” monomers in a half unit cell or across a dimer wall, “oval-shaped” dimer across a dimer wall, and “Y-shaped” trimer within a half unit cell on the 7×7 surface. Understanding intermolecular interactions of biologically relevant molecules is fundamentally important to developing bioinspired applications involving nanoscale engineering and biofunctionalization of semiconductor surfaces. To date, no symmetric Y-shaped trimer has ever been reported on any single-crystal surface, metal and otherwise. Observed for the first time, the methionine Y-shaped trimer represents a novel adsorption structure, not only because it results from formation of a remarkably stable planar arrangement of a triple (O···H–O) H-bonded trimolecular ring with 3-fold symmetry, but also because of the near-perfect-match of its occupied space in the 7×7 half unit cell. These triangular rings of H-bonds and their corresponding interaction energies offer new bonding components for molecular self-organization and biofunctionalization. By annealing the Y-shaped trimer above 373–473 K to break the H-bonds, free carboxylic acid groups could be regenerated, thus enabling the trimer to serve as a reusable molecular trap for other biomolecules.

METHODS

The experiments were carried out in a custom-built, five-chamber ultrahigh vacuum system (Omicron Nanotechnology, Inc.), with a base pressure better than 2×10^{-11} mbar, equipped with a variable-temperature scanning probe microscope for atomic-resolution STM imaging and a X-ray photoelectron spectrometer for chemical-state analysis. Details of the experiments and the system have been described elsewhere.³⁴ Briefly, a single-side-polished n-type Si(111) chip (11×2 mm², 0.3 mm thick, with a resistivity of 0.005 Ω cm) was flash-annealed at ~1473 K for 10 s by direct-current resistive heating, after thoroughly outgassed at 673 K overnight. The resulting contaminant-free Si(111)7×7 surface was verified in situ by STM and XPS. In the organic molecular beam epitaxy chamber, the 7×7 surface held at room temperature was exposed to L-methionine vaporized from its powder (99.5% purity, Fluka), with a normal melting point at 550 K, in a low-temperature organic effusion cell (Dr. Ebert, MBE-Komponenten GmbH) held at 403 K.³⁵ The chamber pressure during deposition was 2×10^{-9} mbar and the methionine powder has been outgassed thoroughly overnight at 373 K. The absolute coverage of methionine was determined directly from the STM images for low exposure, for which the 7×7 registry remained visible. We counted the numbers of methionine adspecies in the STM images at these low exposures and estimated the methionine surface number density, assuming the surface number density of the substrate to be that of an unreconstructed Si(111) surface [i.e., 7.83×10^{14} atoms/cm² for 1 monolayer (ML)]. The molecular identity and integrity of the methionine molecules during exposure were verified in situ by using a quadrupole mass spectrometer (Stanford Research Systems, RGA-300) and the corresponding mass spectrum was found to be in good accord with the literature.³⁶ All STM measurements were performed at room temperature in a constant tunneling current mode using an atomically sharp W tip obtained by electrochemical etching.

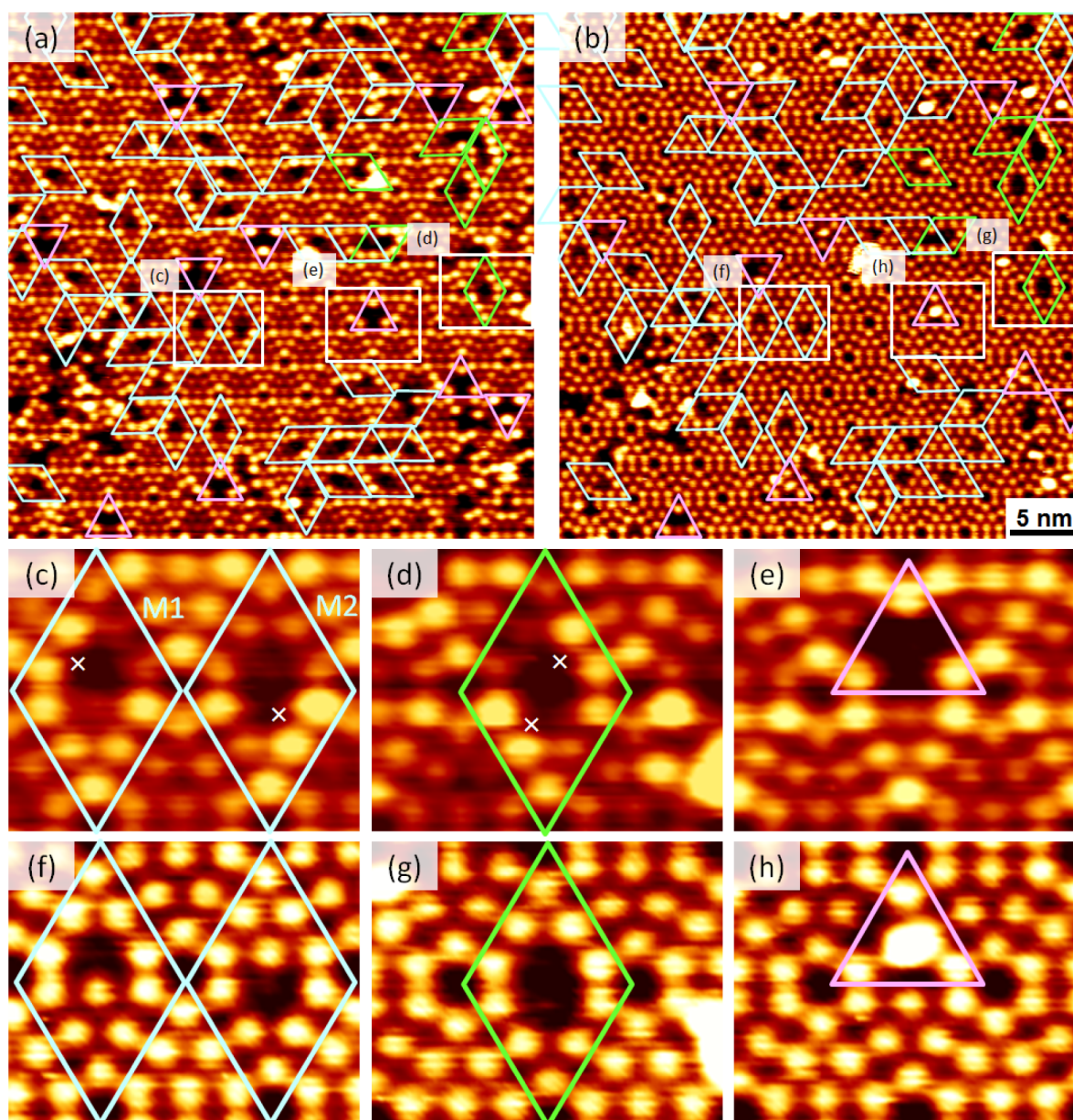


Figure 1. Self-organization of methionine clusters on Si(111)7×7. (a) Filled-state and (b) empty-state STM images (35×35 nm²) for 0.01 ML coverage of L-methionine on Si(111)7×7 obtained with sample bias of −1.7 and +1.7 V, respectively, and a tunneling current of 0.2 nA; and magnified views (6×5 nm²) of filled-state images for (c) monomer “delta” dark depression features, (d) dimer “oval” dark depression feature, and (e) trimer “Y” dark depression feature, along with their corresponding empty-state images shown in (f), (g), and (h), respectively. The locations of the dissociated H atoms are marked by crosses in (c) and (d). In (a) and (b), the unit cells containing methionine monomers and dimers are marked by light cyan and green diamonds, respectively, while the faulted and unfaulted half unit cells containing the trimers are marked by light magenta up and down triangles, respectively.

The DFT-D2 calculations³⁷ were based on the exchange-correlation functional and projector augmented-wave (PAW) potentials,^{38,39} with the inclusion of van der Waals interactions. Full structural optimization using the generalized gradient approximation,^{40,41} as defined by Perdew, Burke, and Ernzerhof (GGA-PBE),⁴² was performed for L-methionine molecules adsorbed on a model Si(111)7×7 surface as represented by a Si₂₀₀H₄₉ slab using the dimer-atom-stacking fault (DAS) model.^{3,43} All five layers of Si atoms and all of the methionine molecules were relaxed until the total residual force was below 0.01 eV/Å using the conjugate-gradient algorithm. The Vienna Ab initio Simulation Package (VASP, version 5.3.3)^{44–46} with

the MedeA platform (Materials Design) was used to implement the calculations.

RESULTS AND DISCUSSION

In our recent X-ray photoelectron spectroscopy (XPS) study on L-methionine on the Si(111)7×7 surface (Supporting Information, Figure S1), we observe N–H dissociative adsorption of a methionine molecule through a dehydrogenated amino group, producing a unidentately N-bonded adspecies (along with a dissociated H atom) in the interfacial layer (the first adlayer). To further investigate specific adsorption geometries of methionine on various 7×7 sites, we conduct STM studies for the early growth stage of the

interfacial layer. Figure 1 shows the filled-state and empty-state STM images ($35 \times 35 \text{ nm}^2$) collected, respectively, at -1.7 and $+1.7 \text{ V}$ sample bias with a 0.2 nA tunneling current, for a 0.01 ML coverage (corresponding to a 5 s exposure) of methionine on $\text{Si}(111)7 \times 7$ at room temperature. Three dark depression features with “delta”, “oval”, and “Y” shapes can be identified on the 7×7 surface registry from the filled-state image (Figure 1a). Dark depression features usually correspond to saturation of the dangling bond sites in a similar way as adsorbed organic molecules such as multicyclic aromatic molecules or long-chain dienes.^{8,19–21} Figure 1c shows that there are two distinct delta features for the darkest depression within a half unit cell, each with a less dark depression feature on the other (complementary) half unit cell. We attribute the first delta feature M1 to a monomer localized at a center adatom (denoted as CA here) entirely within a half unit cell, the presence of which causes the intensity depression at the center adatom across the dimer wall. The brighter appearance of the center adatom and corner adatom (denoted as AA here) on the left of the delta feature is due to reverse charge transfer from the restatom (denoted as RA here) at which adsorption of the dissociated H atom occurs. The second delta feature M2 can be assigned to a monomer bonded to a center adatom with part of the adspecies overhanging the dimer wall. The overhanging moiety undergoes long-range interaction with the center adatom across the dimer wall, which causes the observed depression in the adjacent half unit cell (that appears darker than the corresponding depression for M1). Similarly, the brighter center adatom and corner adatom on the right side of the M2 delta feature is caused by adsorption of the dissociated H atom at the restatom. Evidently, the corresponding empty-state image (Figure 1f) shows a “ Λ -shaped” depression feature (a missing bright spot) at the center adatom for both M1 and M2 delta depression features (Figure 1c). The localization of the Λ -shaped empty-state feature at a single center adatom site (Figure 1f) confirms the covalent bonding interaction from a single methionine monomer adspecies. These two features, M1 and M2, are found on both faulted and unfaulted half unit cells, with the faulted half unit cell being more populated than the unfaulted half unit cell by these monomer features (Figure 1a).

The oval depression feature shown in Figure 1d may be considered as an overlap of two M1 delta features, each located at the adjacent center adatom across the dimer wall in the unit cell. We can also identify the adsorption sites of the dissociated H atoms at the two restatoms next to the respective pairs of brighter protrusions at the center adatom and corner adatom. The corresponding empty-state image (Figure 1g) also shows an oval-shaped depression (located at the two center adatom sites) surrounded by eight equally bright protrusions at neighboring adatom sites. These oval features can therefore be attributed to methionine dimer consisting of two monomers unidentately bonded at center adatoms, likely in the M1 configuration, in adjacent half unit cells.

Similarly, the filled-state Y depression feature shown in Figure 1e can be regarded as a combination of three M2 delta features, each located at the center adatom of a half unit cell. The discernibly minor intensity reduction at the center adatom across the dimer wall in the adjacent half unit cell is consistent with part of the monomer moiety “overhanging” on the other side of the dimer wall. In the corresponding empty-state image (Figure 1h), a large bright protrusion at the center of the half unit cell is connected to three smaller bright protrusions at the apexes of the half unit cell, forming a three-point-star

configuration within the half unit cell. The 3-fold symmetry of both the filled-state and empty-state images indicates the presence of three methionine molecules symmetrically organized in the form of a trimer, located at the center of the half unit cell. As expected, the population of the oval (dimer) features is found to be generally less than the monomer features. Interestingly, the population for the Y (trimer) features is larger than that of the dimer features but less than that of the monomer features, which suggests that the observed anomalous stability could result from the formation of trimer. In the aforementioned STM studies reported to date, only a random distribution of chainlike horseshoe arrangements has been found for cyclic aromatic molecules (benzene, toluene, thiophene, pyrrole, and naphthalene) on various adatom sites and for large diene molecules (1,7-octadiene and 1,13-tetradecadiene) on pairs of various adatom sites. Moreover, amino acids and DNA bases with capability to form intermolecular hydrogen-bonding are found to arrange in higher-order multimer horseshoe configurations (cysteine), dimer configurations (glycine), and self-alignment dimer chains (adenine). Recently, the adsorption of a synthesized molecule [4-methoxy-*N*-(3-sulfonatopropyl) pyridinium] has also been reported to form a triangular trimolecule nanostructure that is bound electrostatically through the S atoms to three restatom sites in a 7×7 half unit cell.²⁷ DFT calculations further suggest that the interaction between 4-methoxy-*N*-(3-sulfonatopropyl) pyridinium (considered as a model zwitterion) and the substrate is driven by electrostatic forces. These weak interactions are consistent with the low desorption temperature of these triangular nanostructures of $\sim 375 \text{ K}$. In contrast, the methionine Y trimers are found to be considerably more stable and stay on the surface until 550 K (Supporting Information, Figure S2). This unusual stability is due to the formation of N–Si bonds in the adsorbed methionine moieties of the trimer and is not found in any of the previously reported self-assembled zwitterionic nanostructures. More importantly, the trimer appears to be dimensionally commensurate with the 7×7 half unit cell. Together with the anomalous stability, the geometrical commensurability with the half unit cell makes the methionine trimer the first “perfect-match” supported cluster observed to date. Furthermore, this is also the first observation of a hybrid organic–inorganic lock-and-key system, where the Y trimer (key) fits perfectly with the 7×7 half unit cell (lock).

While free methionine monomers, dimers, and trimer are chiral, we have not observed the mirror image of the other reflected Y-shaped trimer (in a mirror plane on the other half unit cell). The only example of chirality on $\text{Si}(111)7 \times 7$ surface at room temperature is the self-assembled structures of zwitterionic organic dipoles [4-methoxy-4'-(3-sulfonatopropyl) stilbazolium (MSPS)].⁴⁷ The two observed weak interactions involve very small electronic transfers from the sulfonate groups to the corner adatoms and from the methoxy moieties to Si atoms, which suggests that there is no direct bond formation between any single oxygen atom and a silicon adatom. These weak interactions lead to self-assembly of three MSPS molecules (3-fold star) on the faulted half unit cell and to that of a mirror image of the other reflected three MSPS molecules in a mirror plane on the other half unit cell. This means that the 3-fold stars are chiral, even though free MSPS molecule is achiral. In the case of adsorption of methionine on $\text{Si}(111)7 \times 7$, there is strong covalent interaction, instead of (weak) electrostatic interaction, between the adsorbed methionine and Si surface. The formation of other enantiomers

of Y-shaped trimer by clockwise or anticlockwise folding is not observed for the current coverage of methionine (0.01 ML).

A statistical analysis of multiple STM images obtained from different areas (for example, of approximately 165 7×7 unit cells, including both unpopulated 7×7 unit cells and populated 7×7 unit cells by monomers, dimers, and trimers features) shows that there are more depression features at the center adatoms (with 10% occupancy of all the center adatom sites) than the corner adatoms (0%) and on the faulted half unit cell (21%) than the unfaulted half unit cell (15%). In the 7×7 reconstruction, the restatom and corner-hole sites have a -1 formal charge each, while the formal charge of the adatom site is $+7/12$. Since each center adatom is surrounded by two restatoms instead of only one restatom for the corner adatom, the electron density of the center adatom is therefore lower than the corner adatom.^{48,49} Consequently, the higher reactivity of the center adatom than the corner adatom accounts for the observed higher occupancy of all features at the center adatom sites. Similarly, the higher electrophilicity of the adatom sites on the faulted half unit cell than that on the unfaulted half unit cell may explain the observed greater occupancy on the faulted half unit cell.

To further investigate the nature and orientation of the methionine adspecies on specific 7×7 sites, we evaluate the corresponding line profiles of the local density of states (LDOS) of a delta, an oval, and a Y feature (Supporting Information, Figure S3). The LDOS profiles reveal that (a) reacted center adatom (CA'), where a prime is used here to designate Si atoms in the unfaulted half unit cell) in the reacted half unit cell can no longer be seen because of saturation of the dangling bond with the anchored methionine adspecies; and (b) the adsorption of the dissociated H atom at the restatom site in the reacted half unit cell may cause a reverse charge transfer from RA' back to the surrounding adatoms (Supporting Information, Figure S3a). To determine plausible adsorption geometries for the M1 and M2 delta features and to understand the nature of the interactions between the methionine monomer adspecies and the surface, we conduct large-scale DFT-D2 calculations. Our recent XPS study of methionine adsorption on Si(111) 7×7 has shown that methionine undergoes N–H dissociative adsorption on the 7×7 surface, resulting in N–Si bond formation through the dehydrogenated amino group (Supporting Information, Figure S1). We therefore put an isolated dehydrogenated methionine molecule on various “test” combinations of selected 7×7 sites (e.g., CA and AA in both faulted and unfaulted half unit cells, and also across the dimer wall), with the dissociated H atom located appropriately at a nearest restatom site. Optimized equilibrium geometries and their corresponding adsorption energies are then obtained from the DFT-D2 calculations (Supporting Information, Figure S4). As a methionine adspecies could adopt a wide variety of orientations with respect to the 7×7 surface site registry, a selection of the most stable adsorption configurations over a total of 20 test configurations is made on the basis of their optimized total energies. Among the calculated adsorption configurations that involve bonding through the dehydrogenated amino group with the rest overhanging across the dimer wall, the geometry with the S atom closest to the CA' site across the dimer wall (Figure S4a1, with a separation of 2.55 Å between S and Si adatom) is 0.189 and 0.335 eV more stable than that with the molecular plane (the plane containing the C–S–C backbone) near parallel (Figure S4a2, with a S-to-CA' separation of 4.26 Å) and

near perpendicular to the Si adatom surface plane (Figure S4a3, with a S-to-CA' separation of 5.12 Å), respectively. For other unidentate configurations that involve methionine adspecies bonding completely within a half unit cell, the configuration with the S atom atop of the Si restatom gives the most stable geometry (Figure S4b1, with a separation of 2.33 Å between S and Si restatom), with its adsorption energy 0.224 eV lower than the unidentate configuration across the dimer wall (Figure S4a1). Among the calculated adsorption configurations considered here, the geometry with the S atom closest to a Si adatom or restatom (Figure S4), that is, with the shortest S-to-CA', S-to-CA, or S-to-RA separation, is found to be more stable than other configurations.

For the M1 delta depression feature (Figure 2a), our large-scale DFT-D2 calculation therefore shows that the most favorable adsorption configuration of methionine monomer adspecies within a half unit cell corresponds to a dehydrogenated methionine N-bonded to the center adatom with its S

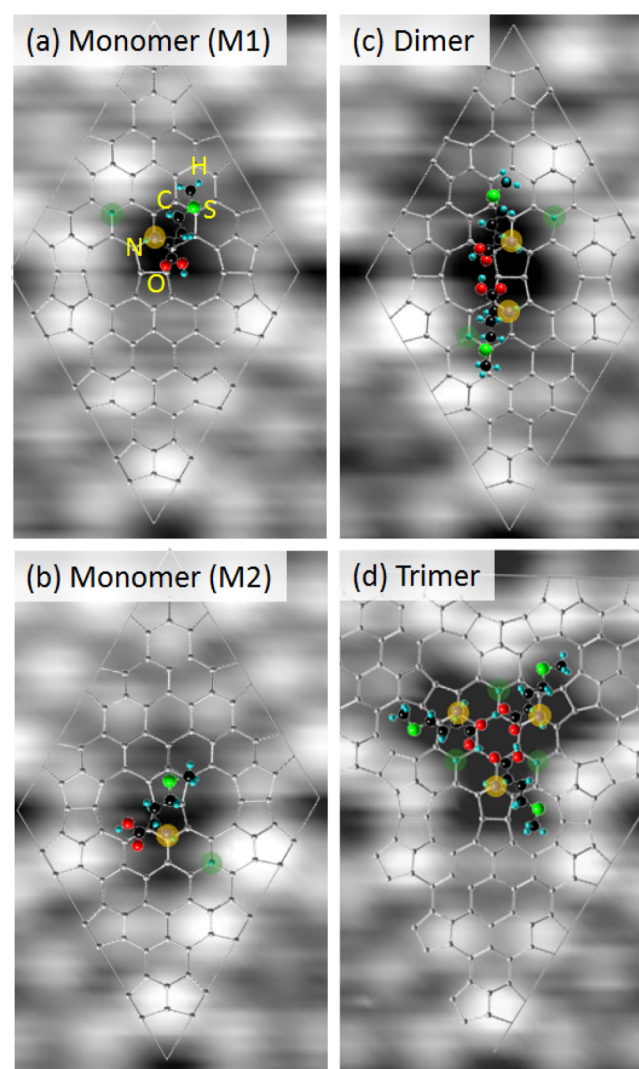


Figure 2. DFT-D2 equilibrium configurations of methionine adspecies on Si(111) 7×7 . Overlays of the most stable equilibrium configurations of methionine adspecies obtained by DFT-D2 calculations on (a) M1 and (b) M2 “delta”, (c) “oval”, and (d) “Y-shaped” dark depression features of the STM filled-state images. For clarity, only the topmost Si layer is shown. Reacted Si center adatoms and restatoms are highlighted by larger yellow and green circles, respectively.

atom undertaking long-range interaction with a restatom through the lone-pair electrons, along with the dissociated H atom on the other restatom site in the same half unit cell (Figure S4b1). The M2 delta depression feature (Figure 2b) then corresponds to the second most stable configuration (Figure S4a1), which involves a dehydrogenated methionine N-bonded to a center adatom in a half unit cell with long-range interaction between the S atom and a center adatom in an adjacent half unit cell across the dimer wall, along with the dissociated H atom on a restatom in the first half unit cell. This overhang of the M2 configuration over the adjacent half unit cell (Figure 2b) accounts for the discernibly darker depression in the adjacent half unit cell when compared with the M1 configuration (Figure 2a). Our previous STM and XPS studies on L-cysteine adsorption on Si(111)7×7 at a very low coverage have supported dissociative adsorption via the amino and thiol functional groups to form a bidentate adsorption configuration across the dimer wall.²⁴ Unlike cysteine, dissociative adsorption via the $-\text{CH}_2-\text{S}-\text{CH}_3$ group in methionine is not possible (Supporting Information, Figure S1). The S atom in methionine could, however, still be sufficiently nucleophilic to exert long-range interaction with an electrophilic site (such as CA). Although the calculated adsorption energy for the M1 configuration located at the corner adatom (-5.544 eV, Figure S4b5) is only slightly less negative than that located at the center adatom (-5.573 eV, Figure S4b1) but is discernibly more negative than the M2 configuration (-5.349 eV, Figure S4a1), we do not observe any M1-like or M2-like delta features located at a corner adatom (for this early growth stage) by STM. The higher electron charge of the center adatom than the corner adatom makes the center adatom more reactive and therefore provides a “kinetically favored” mechanism for the initial adsorption.

For the oval depression feature that covers two center adatom sites across the dimer wall (Supporting Information, Figure S3b), the LDOS line profile of the reacted unit cell clearly shows missing LDOS at the CA and CA' sites, with the dissociated H atoms adsorbed on the respective nearest RA and RA' sites. Our DFT-D2 calculation for the oval feature shows that the most stable dimer corresponds to adsorption of two dehydrogenated methionine adspecies at adjacent CA and CA' sites across the dimer wall (Figure S5b). This dimer is formed by a single $\text{O}\cdots\text{H}-\text{O}$ H-bond between two vicinal carboxylic acid groups of two dehydrogenated methionine adspecies. Interestingly, a slightly more stable calculated dimer configuration, consisting of two dehydrogenated methionine at CA and AA' sites diagonally across the dimer wall and held together by two $\text{O}\cdots\text{H}-\text{O}$ H-bonds (Figure S5a), is not supported by our STM data. This is consistent with our hypothesis that the lower electron charge at the corner adatom than the center adatom makes the corner adatom less reactive and therefore less kinetically favored for the initial adsorption. An overlay of the most probable dimer structure on the oval feature is shown in Figure 2c.

The LDOS profiles for the Y feature illustrate deficit at the CA' sites of the reacted half unit cell, each with a dissociated H atom adsorbed at an adjacent RA' site, which causes a reverse charge transfer from RA' back to a neighboring CA' site (Supporting Information, Figure S3c). Our ultra-large-scale DFT-D2 calculations suggest trimer formation of methionine adspecies within the unfaulted half unit cell. Unlike the calculations for the monomer and dimer features where we use only one $\text{Si}_{200}\text{H}_{49}$ slab, we employ a supercell of four $\text{Si}_{200}\text{H}_{49}$

slabs, that is, a $\text{Si}_{800}\text{H}_{196}$ cluster, as a model for the 7×7 surface, and then strategically position three methionine adspecies and their corresponding dissociated H atoms at the respective CA' and RA' sites. The present ultra-large-scale calculation involving over 1000 atoms therefore represents the largest quantum simulation reported for this surface to date, and it provides us with a reliable, precise quantum-mechanical platform to investigate site-specific chemistry of important proteinogenic biomolecules on the 7×7 surface for the first time. Each methionine adspecies is covalently N-bonded to the Si center adatom site through the dehydrogenated amino group, with the carboxylic acid group pointing toward the center of the half unit cell and the thiol ether group toward the dimer wall (Figure S6, Supporting Information). Interestingly, this molecular orientation is in marked contrast to the M1 monomer (Figure 2a) and dimer adsorption configurations (Figure 2c), in which the carboxylic acid group is pointed toward the dimer wall and the thiol ether group toward the center. It is compelling to suggest that the combination of three M2 monomers (with the surface orientation opposite in alignment to that of M1, Figure 2b) in a single half unit cell leads to the formation of the Y trimer (Figure 2d). With the free carboxylic acid groups of three methionine adspecies pointing toward the center of the half unit cell, formation of triple $\text{O}\cdots\text{H}-\text{O}$ hydrogen bonding is possible. This enables the creation of a cyclic ring structure that significantly stabilizes the adsorption geometry. Remarkably, the cyclic ring structure appears to be commensurate and in near-perfect registry with the 7×7 half unit cell. Figure 2d shows the excellent match of an overlay of this calculated configuration of methionine trimer in the 7×7 half unit cell with the corresponding STM image.

CONCLUSIONS

Methionine chemisorbed on Si(111)7×7 at room temperature under ultrahigh vacuum condition has been studied by combining high-resolution STM images (and XPS results) with large-scale DFT-D2 calculations. Both filled-state and empty-state STM images reveal surface clustering of monomers (delta features) to dimer (oval feature) and trimer (Y feature) at very low methionine coverage. Large-scale DFT-D2 calculations attribute the two delta features to coexistence of two N–Si bonded monomer configurations within a half unit cell on CA (M1) and with overhang across the dimer wall on CA' (M2), along with the respective dissociated H atoms located on RA and RA' sites. A dimer configuration of two methionine adspecies across the dimer wall containing a single $\text{O}\cdots\text{H}-\text{O}$ H-bond between two vicinal carboxylic acid groups corresponds to the oval feature. The Y feature corresponds to a methionine trimer formed with three methionine adspecies in a ring configuration within a 7×7 half unit cell. This is an important result, because not only is this covalently anchored methionine Y trimer observed for the first time, this supported methionine Y trimer also appears to be geometrically and dimensionally in near perfect-match with the surface registry of the 7×7 half unit cell. We also employ the largest DFT-D2 calculations reported to date, which involve over 1000 atoms, as the new quantum-mechanical platform to model this Y trimer and other supported clusters on the 7×7 surface. Our ultra-large-scale DFT-D2 calculation shows that the Y trimer is driven by the formation of three $\text{O}\cdots\text{H}-\text{O}$ hydrogen bonds, in a ring configuration, among the unattached carboxylic acid groups from three methionine adspecies that are covalently attached to the Si center adatom sites via the N–Si bond. In

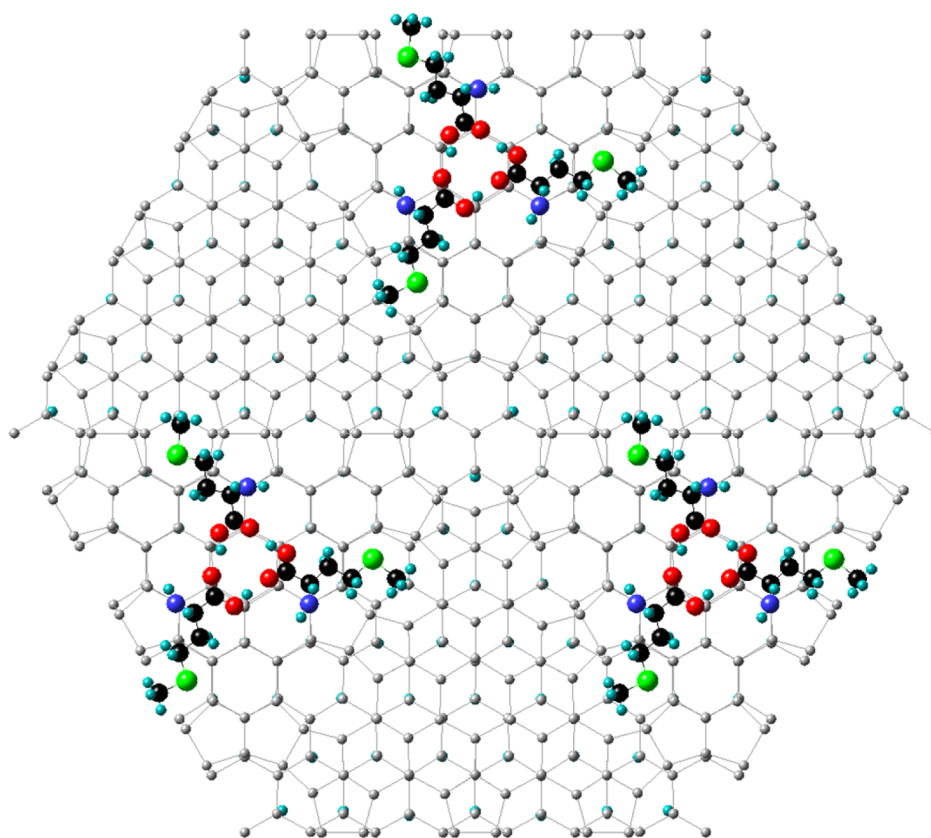


Figure 3. Schematic model of a nanopattern formed by L-methionine Y-shaped trimers on Si(111)7×7.

marked contrast to the zwitterionic structures reported for other molecules, the unique combination of covalent and hydrogen bonding in this configuration accounts for the anomalous stability of the trimer (up to 550 K). Figure 3 shows a model of Y trimers supported on Si(111)7×7 surface envisioned for plausible applications: (a) as a hybrid organic–inorganic lock-and-key system, where the Y trimer (key) fits perfectly with the 7×7 half unit cell (lock) to provide biopassivation of the center adatom sites; (b) as a molecular mask for nanopatterning to block the highly reactive Si center adatom sites, thus allowing the corner adatom sites to react selectively with other adspecies, and (c) as a recyclable molecular trap by breaking the hydrogen bonding above 373 K to free the carboxylic acid groups to catch-and-release other molecules at appropriate temperature. Fundamental studies of site-specific interfacial chemistry, including molecular orientation and self-organization, of methionine adspecies on the Si(111)7×7 surface are therefore useful not only to understanding the growth of component biomolecules into organized nanoarchitectures at the molecular level but also to design of biosensors, drug delivery carriers, and bioinspired nanosystems and appliances.

■ ASSOCIATED CONTENT

📄 Supporting Information

The Supporting Information is available free of charge on the ACS Publications website at DOI: 10.1021/acs.jpcc.5b11649.

XPS analysis and line profiles of the local density of states of methionine (PDF)

■ AUTHOR INFORMATION

Corresponding Author

*Email: tong@uwaterloo.ca. Tel: 519-888-4567 ext. 35826.

Author Contributions

F.R.R. and K.T.L. contributed to the concept and design of the study. F.R.R. performed the STM and XPS experiments and data analysis and the large-scale DFT-D2 calculations. F.R.R. and K.T.L. wrote the paper.

Notes

The authors declare no competing financial interest.

■ ACKNOWLEDGMENTS

This work was supported by the Natural Sciences and Engineering Research Council of Canada.

■ REFERENCES

- (1) Tao, F.; Bernasek, S. L. *Functionalization of Semiconductor Surfaces*; John Wiley & Sons, Inc.: Hoboken, NJ, 2012.
- (2) Leftwich, T. R.; Teplyakov, A. V. Chemical Manipulation of Multifunctional Hydrocarbons on Silicon Surfaces. *Surf. Sci. Rep.* **2008**, *63*, 1–71.
- (3) Takayanagi, K.; Tanishiro, Y.; Takahashi, M.; Takahashi, S. Structural Analysis of Si(111)7×7 by UHV Transmission Electron Diffraction and Microscopy. *J. Vac. Sci. Technol., A* **1985**, *3*, 1502–1506.
- (4) Binnig, G.; Rohrer, H.; Gerber, C.; Weibel, E. 7×7 Reconstruction on Si(111) Resolved in Real Space. *Phys. Rev. Lett.* **1983**, *50*, 120–123.
- (5) Binnig, G.; Rohrer, H.; Gerber, C.; Weibel, E. Surface Studies by Scanning Tunneling Microscopy. *Phys. Rev. Lett.* **1982**, *49*, 57–61.
- (6) Yoshinobu, J.; Fukushi, D.; Uda, M.; Nomura, E.; Aono, M. Acetylene Adsorption on Si(111)(7×7): A Scanning-Tunneling-

Microscopy Study. *Phys. Rev. B: Condens. Matter Mater. Phys.* **1992**, *46*, 9520–9524.

(7) Piancastelli, M. N.; Motta, N.; Sgarlata, A.; Balzarotti, A.; De Crescenzi, M. Topographic and Spectroscopic Analysis of Ethylene Adsorption on Si(111)7×7 by STM and STS. *Phys. Rev. B: Condens. Matter Mater. Phys.* **1993**, *48*, 17892–17896.

(8) Shachal, D.; Manassen, Y.; Ter-Ovanesyan, E. Role of Chain Length on the Surface Chemistry of Dienes Studied by Scanning Tunneling Microscopy. *Phys. Rev. B: Condens. Matter Mater. Phys.* **1997**, *55*, 9367–9370.

(9) Baik, J.; Kim, M.; Park, C.-Y.; Kim, Y.; Ahn, J. R.; An, K.-S. Cycloaddition Reaction of 1,3-Butadiene with a Symmetric Si Adatom Pair on the Si(111)7×7 Surface. *J. Am. Chem. Soc.* **2006**, *128*, 8370–8371.

(10) Kawasaki, T.; Sakai, D.; Kishimoto, H.; Akbar, A. A.; Ogawa, T.; Oshima, C. Adsorption and Desorption of Benzene on Si(111)-7×7 Studied by Scanning Tunneling Microscopy. *Surf. Interface Anal.* **2001**, *31*, 126–130.

(11) Tomimoto, H.; Takehara, T.; Fukawa, K.; Sumii, R.; Sekitani, T.; Tanaka, K. Study of Benzene and Toluene on Si(111)7×7 Surface by Scanning Tunneling Microscopy. *Surf. Sci.* **2003**, *526*, 341–350.

(12) Horn, S. A.; Patitsas, S. N. STM Study of Charge Transfer and the Role of Rest-Atoms in the Binding of Benzene to Si(111)7×7. *Surf. Sci.* **2008**, *602*, 630–637.

(13) Yong, K. S.; Yang, S.-W.; Zhang, Y. P.; Wu, P.; Xu, G. Q. Adsorption-Induced Desorption of Benzene on Si(111)-7×7 by Substrate-Mediated Electronic Interactions. *Langmuir* **2008**, *24*, 3289–3293.

(14) Cao, Y.; Yong, K. S.; Wang, Z. Q.; Chin, W. S.; Lai, Y. H.; Deng, J. F.; Xu, G. Q. Dry Thienylation of the Silicon (111)-(7×7). *J. Am. Chem. Soc.* **2000**, *122*, 1812–1813.

(15) Cao, Y.; Yong, K. S.; Wang, Z. H.; Deng, J. F.; Lai, Y. H.; Xu, G. Q. Cycloaddition Chemistry of Thiophene on the Silicon (111)-7×7 Surface. *J. Chem. Phys.* **2001**, *115*, 3287–3296.

(16) Chatterjee, A.; Zhang, L.; Leung, K. T. Surface [4+2] Cycloaddition Reaction of Thymine on Si(111)7×7 Observed by Scanning Tunneling Microscopy. *J. Phys. Chem. C* **2013**, *117*, 14677–14683.

(17) Guisinger, N. P.; Elder, S. P.; Yoder, N. L.; Hersam, M. C. Ultra-High Vacuum Scanning Tunneling Microscopy Investigation of Free Radical Adsorption to the Si(111)-7×7 Surface. *Nanotechnology* **2007**, *18*, 044011.

(18) Yuan, Z. L.; Chen, X. F.; Wang, Z. H.; Yong, K. S.; Cao, Y.; Xu, G. Q. Dissociative Adsorption of Pyrrole on Si(111)-(7×7). *J. Chem. Phys.* **2003**, *119*, 10389–10395.

(19) Yong, K. S.; Zhang, Y. P.; Yang, S.-W.; Xu, G. Q. Naphthalene Adsorption on Si(111)-7×7. *Surf. Sci.* **2008**, *602*, 1921–1927.

(20) Yong, K. S.; Zhang, Y. P.; Yang, S.-W.; Wu, P.; Xu, G. Q. Studies of Chemisorbed Tetracene on Si(111)-7×7. *J. Phys. Chem. A* **2007**, *111*, 12266–12274.

(21) Yong, K. S.; Zhang, Y. P.; Yang, S.-W.; Wu, P.; Xu, G. Q. Chemisorption of Pentacene on Si (111)-7×7 Studied via Scanning Tunneling Microscopy and Density Functional Theory. *J. Phys. Chem. C* **2007**, *111*, 4285–4293.

(22) Cao, X.; Hamers, R. J. Molecular and Dissociative Bonding of Amines with the Si(111)-(7×7) Surface. *Surf. Sci.* **2003**, *523*, 241–251.

(23) Chatterjee, A.; Zhang, L.; Leung, K. T. Direct Imaging of Hydrogen Bond Formation in Dissociative Adsorption of Glycine on Si(111)7×7 by Scanning Tunneling Microscopy. *J. Phys. Chem. C* **2012**, *116*, 10968–10975.

(24) Rahsepar, F. R.; Zhang, L.; Farkhondeh, H.; Leung, K. T. Biofunctionalization of Si(111)7×7 by “Renewable” L-Cysteine Transitional Layer. *J. Am. Chem. Soc.* **2014**, *136*, 16909–16918.

(25) Chatterjee, A.; Zhang, L.; Leung, K. T. Bidentate Surface Structures of Glycylglycine on Si(111)7×7 by High-Resolution Scanning Tunneling Microscopy: Site-Specific Adsorption via N–H and O–H or Double N–H Dissociation. *Langmuir* **2012**, *28*, 12502–12508.

(26) Chatterjee, A.; Zhang, L.; Leung, K. T. Self-Directed Growth of Aligned Adenine Molecular Chains on Si(111)7×7: Direct Imaging of Hydrogen-Bond Mediated Dimers and Clusters at Room Temperature by Scanning Tunneling Microscopy. *Langmuir* **2013**, *29*, 9369–9377.

(27) El Garah, M.; Makoudi, Y.; Duverger, E.; Palmino, F.; Rochefort, A.; Chérioux, F. Large-Scale Patterning of Zwitterionic Molecules on a Si(111)-7×7 Surface. *ACS Nano* **2011**, *5*, 424–428.

(28) Barlow, S. M.; Raval, R. Complex Organic Molecules at Metal Surfaces: Bonding, Organisation and Chirality. *Surf. Sci. Rep.* **2003**, *50*, 201–341.

(29) Naitabdi, A.; Humblot, V. Chiral Self-Assemblies of Amino-Acid Molecules: D- and L-Methionine on Au(111) Surface. *Appl. Phys. Lett.* **2010**, *97*, 223112.

(30) Humblot, V.; Tielens, F.; Luque, N. B.; Hampartsoumian, H.; Méthivier, C.; Pradier, C.-M. Characterization of Two-Dimensional Chiral Self-Assemblies L- and D-Methionine on Au(111). *Langmuir* **2014**, *30*, 203–212.

(31) Schiffrin, A.; Riemann, A.; Auwarter, W.; Pennec, Y.; Weber-Bargioni, A.; Cvetko, D.; Cossaro, A.; Morgante, A.; Barth, J. V. Zwitterionic Self-Assembly of L-Methionine Nanogratings on the Ag(111) Surface. *Proc. Natl. Acad. Sci. U. S. A.* **2007**, *104*, 5279–5284.

(32) Schiffrin, A.; Reichert, J.; Pennec, Y.; Auwarter, W.; Weber-Bargioni, A.; Marschall, M.; Dell’Angela, M.; Cvetko, D.; Bavdek, G.; Cossaro, A.; et al. Self-Assembly of L-Methionine on Cu(111): Steering Chiral Organization by Substrate Reactivity and Thermal Activation. *J. Phys. Chem. C* **2009**, *113*, 12101–12108.

(33) Kühnle, A. Self-Assembly of Organic Molecules at Metal Surfaces. *Curr. Opin. Colloid Interface Sci.* **2009**, *14*, 157–168.

(34) Rahsepar, F. R.; Zhang, L.; Leung, K. T. Two-Dimensional Self-Assembled Gold Silicide Honeycomb Nanonetwork on Si(111)7×7. *J. Phys. Chem. C* **2014**, *118*, 9051–9055.

(35) Gross, D.; Grodzky, G. On the Sublimation of Amino Acids and Peptides. *J. Am. Chem. Soc.* **1955**, *77*, 1678–1680.

(36) Naumkin, A. V.; Kraut-Vass, A.; Gaarenstroom, S. W.; Powell, C. J. X-Ray Photoelectron Spectroscopy Database. In *NIST Chemistry Webbook*; Linstrom, P. J., Mallard, W. G., Eds.; NIST Standard Reference Database 20, Version 4.1; National Institute of Standards and Technology: Gaithersburg, MD; <http://webbook.nist.gov> (retrieved September 15, 2012).

(37) Grimme, S. Semiempirical GGA-Type Density Functional Constructed with a Long-Range Dispersion Correction. *J. Comput. Chem.* **2006**, *27*, 1787–1799.

(38) Blochl, P. E. Projector Augmented-Wave Method. *Phys. Rev. B: Condens. Matter Mater. Phys.* **1994**, *50*, 17953–17979.

(39) Kresse, G.; Joubert, D. From Ultrasoft Pseudopotentials to the Projector Augmented-Wave Method. *Phys. Rev. B: Condens. Matter Mater. Phys.* **1999**, *59*, 1758–1775.

(40) Wang, Y.; Perdew, J. P. Correlation Hole of the Spin-Polarized Electron Gas, with Exact Small-Wave-Vector and High-Density Scaling. *Phys. Rev. B: Condens. Matter Mater. Phys.* **1991**, *44*, 13298–13307.

(41) Perdew, J. P.; Chevary, J. A.; Vosko, S. H.; Jackson, K. A.; Pederson, M. R.; Singh, D. J.; Fiolhais, C. Atoms, Molecules, Solids, and Surfaces: Applications of the Generalized Gradient Approximation for Exchange and Correlation. *Phys. Rev. B: Condens. Matter Mater. Phys.* **1992**, *46*, 6671–6687.

(42) Perdew, J. P.; Burke, K.; Ernzerhof, M. Generalized Gradient Approximation Made Simple. *Phys. Rev. Lett.* **1996**, *77*, 3865–3868.

(43) Takayanagi, K.; Tanishiro, Y.; Takahashi, S.; Takahashi, M. Structure Analysis of Si(111)-7×7 Reconstructed Surface by Transmission Electron Diffraction. *Surf. Sci.* **1985**, *164*, 367–392.

(44) Kresse, G.; Hafner, J. Ab Initio Molecular Dynamics for Liquid Metals. *Phys. Rev. B: Condens. Matter Mater. Phys.* **1993**, *47*, 558–561.

(45) Kresse, G.; Furthmüller, J. Efficient Iterative Schemes for Ab Initio Total-Energy Calculations Using a Plane-Wave Basis Set. *Phys. Rev. B: Condens. Matter Mater. Phys.* **1996**, *54*, 11169–11186.

(46) Kresse, G.; Furthmüller, J. Efficiency of Ab-Initio Total Energy Calculations for Metals and Semiconductors Using a Plane-Wave Basis Set. *Comput. Mater. Sci.* **1996**, *6*, 15–50.

(47) Makoudi, Y.; Arab, M.; Palmino, F.; Duverger, E.; Ramseyer, C.; Picaud, F.; Chérioux, F. A Stable Room-Temperature Molecular Assembly of Zwitterionic Organic Dipoles Guided by a Si(111)-7×7 Template Effect. *Angew. Chem., Int. Ed.* **2007**, *46*, 9287–9290.

(48) Northrup, J. E. Origin of Surface States on Si(111)(7×7). *Phys. Rev. Lett.* **1986**, *57*, 154–157.

(49) Tao, F.; Xu, G. Q. Attachment Chemistry of Organic Molecules on Si(111)-7×7. *Acc. Chem. Res.* **2004**, *37*, 882–893.